

Available online at [www.sciencedirect.com](http://www.sciencedirect.com)

ScienceDirect

journal homepage: [www.elsevier.com/locate/radcr](http://www.elsevier.com/locate/radcr)

## Case Report

# Fusion imaging of single-photon emission computed tomography and magnetic resonance lymphangiography for post-Fontan chylothorax <sup>☆</sup>

Takashi Shima, MD, PgDip<sup>a,b,\*</sup>, Takuya Hara, MD<sup>c,d</sup>, Keisuke Sato, MD<sup>e</sup>,  
Nobuhiko Kan, MD<sup>a,b,c</sup>, Tadamune Kinjo, MD, PhD<sup>a</sup>

<sup>a</sup>Department of Neonatology, Fukuoka Children's Hospital, 5-1-1, Kashiiteriha, Higashiku, Fukuoka, Fukuoka, 813-0017, Japan

<sup>b</sup>Department of Fetal Cardiology, Fukuoka Children's Hospital, 5-1-1, Kashiiteriha, Higashiku, Fukuoka, Fukuoka, 813-0017, Japan

<sup>c</sup>Department of Cardiology, Fukuoka Children's Hospital, 5-1-1, Kashiiteriha, Higashiku, Fukuoka, Fukuoka, 813-0017, Japan

<sup>d</sup>Department of Pediatrics, Oita Prefectural Hospital, 2-8-1, Bunyo, Oita, Oita, 870-8511, Japan

<sup>e</sup>Department of Cardiology, Shizuoka Children's Hospital, 860, Urushiyama, Aoi Ward, Shizuoka, Shizuoka, 420-8660, Japan

## ARTICLE INFO

## Article history:

Received 23 December 2022

Accepted 7 January 2023

## Keywords:

Cardiology

Chylothorax

Lymphography

MRI

Pediatrics

SPECT

## ABSTRACT

A preschool male patient with an extensive cardiac surgical history developed refractory chylothorax after a total cavopulmonary connection. Neither lymphoscintigraphy nor single-photon emission computed tomography (SPECT)/computed tomography could identify the lymphatic system leakage sites. Non-contrast heavy T2-weighted magnetic resonance lymphangiography (MRL) was performed to visualize the lymphatic system. Nevertheless, distinguishing lymphatic ducts from other watery structures of the patient remained difficult. Therefore, non-contrast MRL and SPECT images were fused. This hybrid diagnostic tool elucidated the pathophysiology of the prolonged chylothorax; pulmonary lymphatic perfusion syndrome and illustrated the anatomical connection of the thoracic duct and an abnormally dilated lymphatic network in the neck and left hilar regions. Subsequent intranodal lymphangiography with ethiodized oil confirmed these findings. SPECT/MRL may become an alternative modality for revealing the mechanism of prolonged chylothorax by visualizing the lymphatic system when dynamic contrast-enhanced magnetic resonance lymphangiography is unavailable.

© 2023 The Authors. Published by Elsevier Inc. on behalf of University of Washington.

This is an open access article under the CC BY-NC-ND license (<http://creativecommons.org/licenses/by-nc-nd/4.0/>)

<sup>☆</sup> Competing Interests: The authors declare that they have no known competing financial interests or personal relationships that could have appeared to influence the work reported in this paper.

\* Corresponding author.

E-mail address: [shima.t@fcho.jp](mailto:shima.t@fcho.jp) (T. Shima).

<https://doi.org/10.1016/j.radcr.2023.01.021>

1930-0433/© 2023 The Authors. Published by Elsevier Inc. on behalf of University of Washington. This is an open access article under the CC BY-NC-ND license (<http://creativecommons.org/licenses/by-nc-nd/4.0/>)

## Introduction

Postoperative chylothorax is a clinical challenge in patients with congenital heart disease (CHD). The pathophysiology of this lymphatic failure remains an enigma due to the lack of reliable tests. In addition, anatomical variants of the thoracic duct (TD) could obstruct surgical interventions [1].

Lymphoscintigraphy (LS) and single-photon emission computed tomography (SPECT)/computed tomography (CT) have been used for lymphatic imaging [2]; however, neither offer a distinct visualization of lymphatic vessels. An intranodal lymphangiogram (IL) involves ultrasound-guided intranodal ethiodized oil contrast injection (Lipiodol, Guerbet Japan, Tokyo, Japan). In addition to its diagnostic value, Lipiodol induces inflammation and saponification, leading to the cessation of lymphatic leakage [3]. Meanwhile, IL is a moderately invasive procedure that can cause vascular embolization in patients with a right-to-left intracardiac shunt [4].

Non-contrast heavy T2 magnetic resonance lymphangiography (MRL) is a novel application of magnetic resonance imaging (MRI) using 3-dimensional sampling perfection with application-optimized contrast using different flip angle evolution (3D-SPACE) [5]. This sequence targets water-rich structures, including lymphatic vessels [6]. The limitations of non-contrast MRL include a lack of lymphodynamic data and difficulty in separating lymphatic ducts from nearby pleural effusions. Furthermore, this modality cannot visualize the major collateral channels, which are essential information for selective embolization, owing to the lack of contrast materials [7]. Dynamic contrast-enhanced magnetic resonance lymphangiography (DCMRL) using T1-weighted 3-dimensional gradient sequences with gadolinium contrast has generated publicity owing to its excellent anatomical resolution with dynamic data [8]. However, its complicated process (ie, ultrasound-guided placement of the intranodal needle outside the magnetic field, followed by patient transfer with unstable needles into the tunnel of the MRI scanner) has hindered its clinical application.

Therefore, the development of alternatives to DCMRL is required. We hypothesized that a hybrid image of SPECT and non-contrast MRL, SPECT/MRL, may substitute DCMRL. We report a case of CHD with refractory chylothorax after total cavopulmonary connection (TCPC), in which SPECT/MRL was successfully used to illustrate the pathophysiology.

The ethics committee of Fukuoka Children's Hospital approved this case report (Permission number: 2022-58).

## Case presentation

A preschool male patient with hypoplastic left heart complex (mitral stenosis–atrial stenosis), right ventricular outflow tract obstruction, and aortic valve regurgitation was hospitalized for cardiac surgery. He had undergone serial cardiac operations, including the Norwood procedure and the bidirectional Glenn procedure.

After admission, the patient underwent TCPC (18-mm Gore-Tex conduit), right ventricular outflow tract muscle re-

section, and aortic valvuloplasty. Subsequently, he developed bilateral refractory chylothorax. Examination of the pleural effusion revealed the following: white blood cells,  $2.05 \times 10^9$  cells/L (91% lymphocytes); total protein, 5.1 g/dL; and triglycerides, 50 mg/dL; these results were consistent with the diagnostic criteria for chylothorax [9]. The patient's daily output ranged from 30 to 80 mL/kg.

Cardiac catheterization 20 days after TCPC revealed a central venous pressure (CVP) of 12 mmHg, an aortic oxygen saturation (SaO<sub>2</sub>) of 96%, a cardiac index (CI) of 3.5 L/min/m<sup>2</sup>, and a pulmonary resistance vascular resistance index (R<sub>pl</sub>) of 2.9 WU·m<sup>2</sup>. The aortopulmonary collateral artery from the inferior phrenic artery was embolized. The chylothorax disappeared after embolization, only to reoccur within a week. Pharmacological treatments (prednisolone, octreotide, factor XIII, and etilefrine) and fat restriction were ineffective.

LS and SPECT were performed using the Symbia E dual-head system (Siemens Medical Solutions, Erlangen, Germany) 52 days after TCPC. A radioactive tracer (Technetium-99m diethylenetriaminepentaacetic acid human serum albumin: 99<sup>m</sup> Tc-DTPA HSA, 85.0 MBq) was subcutaneously injected into each foot, and dynamic imaging was performed for 80 minutes. SPECT images were captured at 80 minutes, which was the segment of the maximal abnormal distribution pattern. SPECT/CT detected abnormal radioactive hotspots in the left lung, hilum, and neck, suggesting lymphatic stagnation at these locations. However, the lymphatic leakage point was obscure (Fig. 1A).

Non-contrast MRL was performed using a 1.5T MAGNETOM Avanto system (Siemens Medical Solutions, Erlangen, Germany) 70 days after TCPC. The parameters of the MRL were as follows: Matrix, 256 × 256; field of view, 400; repetition time/echo time, 4175/650 ms; flip angle, 140°; voxel size, 1.5 × 1.5 × 1.5 mm; and scan time, 5 min. A coronal slice of the non-contrast MRL showed incomplete TD with loss of visualization in the upper part. This finding indicated an impaired or occluded TD (Fig. 2A). Additionally, heterogeneous dendritically expanded T2-weighted structures were observed in the neck and lung hilum (Fig. 2B). Although the appearances were like pulmonary lymphangiectasia, also known as “nutmeg lung,” on fetal MRI [10], it was difficult to distinguish the findings from other water-rich structures.

Postoperative chylothorax has 3 types of etiology in patients with CHD: (1) laceration of the TD; (2) pulmonary lymphatic perfusion syndrome (PLPS); and (3) central lymphatic flow disorder (CLFD) [11,12]. PLPS is a countercurrent lymphatic flow from the TD to the pulmonary system, through an abnormal lymphatic network. Meanwhile, CLFD refers to a multicompartiment lymphatic abnormality that involves the chylopericardium, chyloascites, and dermal backflow on the abdominal wall. CLFD is also characterized by occlusion or dysplasia of the TD from the viewpoint of TD anatomy. Although DCMRL was considered an ideal modality for a detailed examination in this case, we had no capacity to perform DCMRL due to lack of experience at this time. Therefore, SPECT was combined with MRL to accentuate the lymphatic pathway as a workaround. SPECT/MRL helped rule out lymphatic flow interruption in the middle of the TD based on the lack of stagnation of radioactive tracers at the point

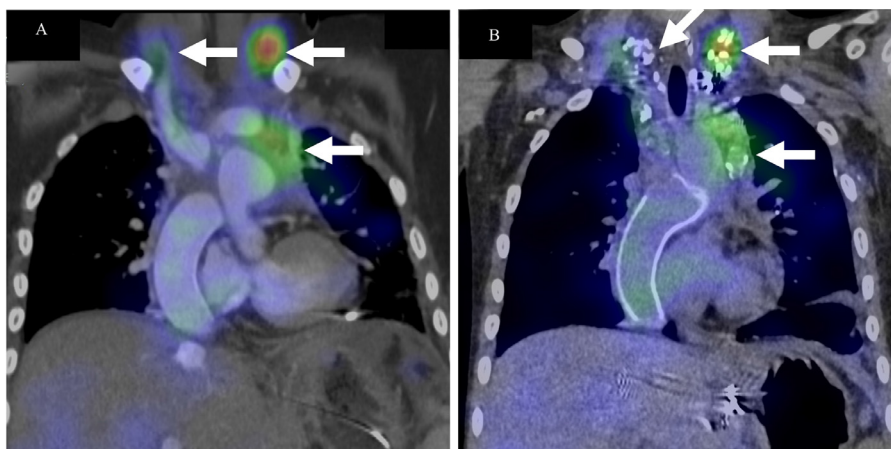


**Fig. 1 – SPECT/CT of the thorax.** The strength of radioactivity is shown in the order of orange, yellow, and green. (A) Imaging demonstrates tracer holdup in the left lung, hilum, and neck (white arrows). (B) SPECT/CT after intranodal lymphangiography shows the coincidence of radioactive hotspots and infused contrast materials (white arrows).

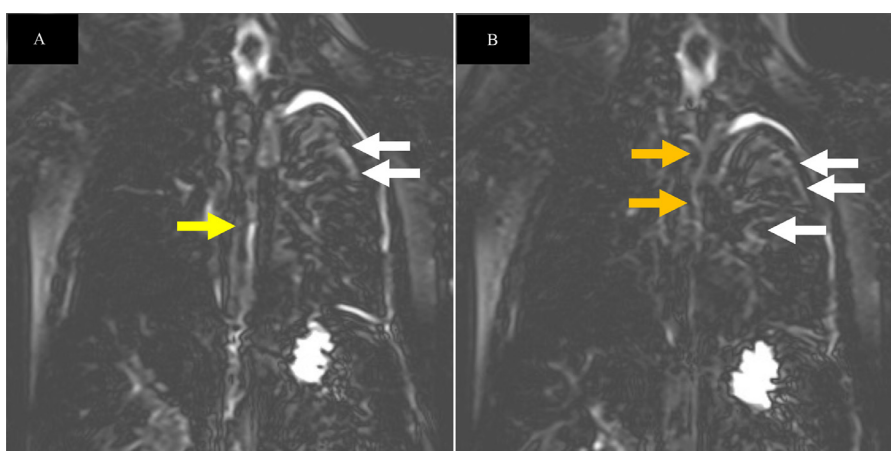


**Fig. 2 – Non-contrast magnetic resonance lymphangiography of the thorax.** (A) The thoracic duct (TD) in a slice of coronal view appears to show flow disruption (yellow arrow), masquerading as impairment or occlusion of TD. (B) TD (orange arrows), and T2 hyperintense dendritic structures (white arrows) within the lung parenchyma are described in the other slice.

where the occlusion was suspected in the non-contrast MRL (Fig. 3A). Moreover, the overlapped radioactive tracers on the nutmeg-like findings elucidated the lymphatic connection of the TD and abnormal lymphatic dilatation in the cervical and left hilar lung areas (Fig. 3B). SPECT/MRL findings suggested PLPS, and the results of cardiac catheterization indicated the hemodynamic profile of the patient were inconsistent with a failing Fontan circulation [13].

Based on the discussion, the patient was not indicated for Fontan takedown, and IL preceded TD ligation. Unfortunately, operators who could perform percutaneous lymphatic embolization were unavailable, partially due to the COVID-19 pandemic. As a suboptimal choice, IL using Lipiodol at a dose of 0.3 mL/kg was performed, and the bubbly contrasts flowed into the left pleural cavity and the bilateral cervical regions (Fig. 4, Supplementary video). These findings were consistent with those of SPECT/MRL (Fig. 3). For reference, SPECT 52 days

after TCPC and CT after IL were combined and showed the coincidence of radioactive tracers and pooled ethiodized oil in the neck and left lung hilum (Fig. 1B).

The postoperative course was uneventful, and the chylothorax resolved. Eventually, the patient was discharged from the hospital 1 month after IL, following a 6-month hospital stay.

## Discussion

In this case report, 4 types of imaging studies were compared: SPECT/CT (Figs. 1A and B), non-contrast MRL (Fig. 2B), SPECT/MRL (Fig. 3), and IL (Fig. 4). The findings depicted in Figs. 1B and 4 were considered definitive results based on the presence of contrast material in the lymphatic vessels. This

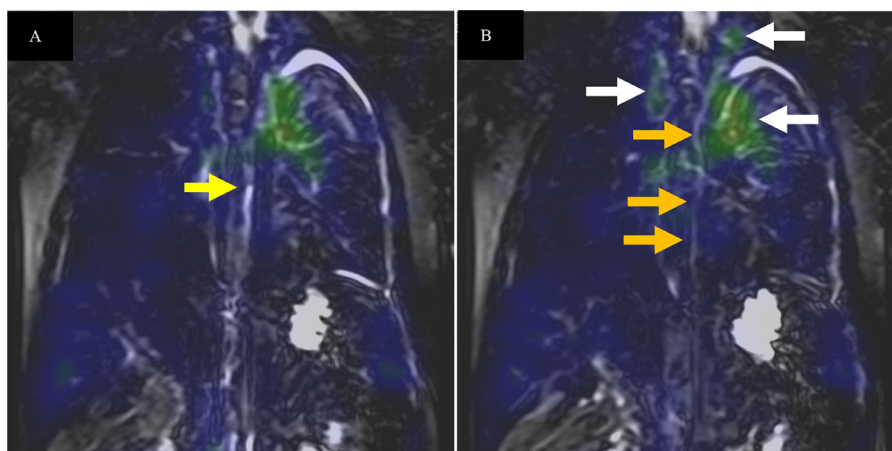


**Fig. 3 – Fusion imaging of SPECT and magnetic resonance lymphangiography of the thorax. (A) Flow disruption is ruled out because of the absence of radioactive tracers in the midstream of the thoracic duct (yellow arrow). (B) The thoracic duct (orange arrows) is connected to the lymphangiectasia in the neck and lung hilum, highlighted by the tracers (white arrows).**

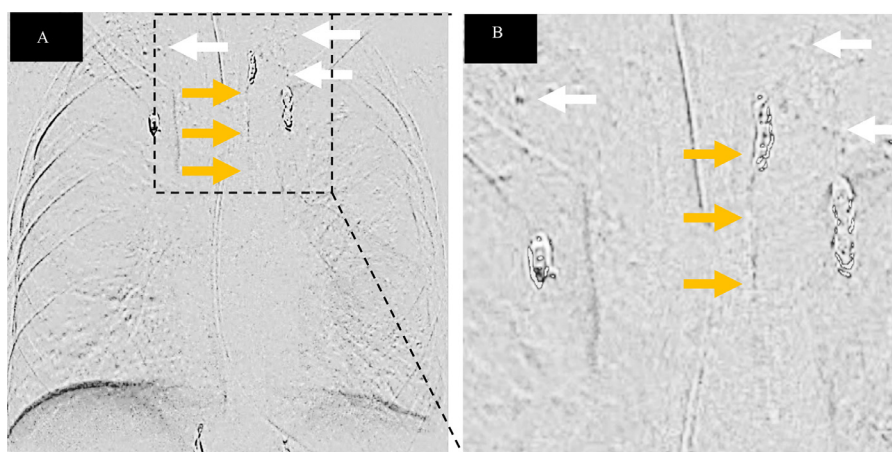


**Fig. 4 – Intranodal lymphangiography (IL) of the thorax. (A) IL using the digital subtraction angiography technique. (B) The magnified IL image in the superior mediastinum. Contrast bubbles in the thoracic duct (orange arrows) that flow into the left thoracic cavity and parasubclavian areas (white arrows).**

comparison revealed that SPECT/MRL successfully illustrated the pathophysiology of prolonged chylothorax in this patient.

“Failing Fontan circulation” is a term commonly used in clinical settings, but its definition is still uncertain. The hemodynamic characteristics of Failing Fontan anecdotally include elevated CVP, decreased cardiac output, and decreased SaO<sub>2</sub>, although there is no numerical threshold for each parameter [13]. In our case, the results of cardiac catheterization (ie, CVP of 12 mmHg, CI of 3.5 L/min\*m<sup>2</sup>, and SaO<sub>2</sub> of 96%) were inconsistent with the characteristics of Fontan failure. SPECT/CT (Fig. 1B) and SPECT/MRL (Fig. 3) showed lymphangiectasia in the superior mediastinum near the orifice of the TD, suggesting lymphatic congestion after TCPC [14]. Fontan failure is categorized based on the following clinical phenotypes: type 1, systolic ventricular dysfunction; type 2, diastolic ventricular dysfunction; type 3, normal hemodynamics; and type 4, lymphatic abnormalities [15]. Therefore, refractory lymphorrhoea after TCPC can be a symptom of Failing Fontan

circulation, even if the hemodynamic characteristics of the patient on catheter examination appear normal. Our case exemplifies the coexistence of type 3 and type 4 Failing Fontan circulations. Lymphatic abnormalities on MRI and prolonged chylothorax can predict unfavorable short and medium-term outcomes including death, Fontan takedown, plastic bronchitis, and protein-losing enteropathy [5,16]. Therefore, SPECT/MRL may serve as a predictive tool for identifying several complications related to the Fontan circulation.

The anatomy of the TD plays a pivotal role in explaining the mechanism of lymphorrhoea and determining therapeutic options. A typical TD arises from the cisterna chyli and proceeds to the right descending aorta. Then it crosses the left and drains into the left venous angle. However, only half of the patients had typical TD. Knowledge of the course of TD is essential for effective surgical interventions [1]. Besides, invasive lymphatic interventions can disrupt the equilibrium of the lymphatic system in patients with CLFD [12]. Therefore, a

detailed evaluation of lymphatic anatomy is necessary prior to TD ligation or percutaneous lymphatic embolization.

SPECT/MRL uses anatomical information from non-contrast MRL instead of CT, and the integration of SPECT and MRL was performed on a commercial workstation (SYNAPSE VINCENT, Fujifilm, Tokyo, Japan). Some studies have shown the usefulness of SPECT/MRI in highlighting the lymphatic system, including sentinel lymph nodes [17,18]. However, there is little information on the application of SPECT/MRL in chylothorax.

SPECT/MRL has several limitations in SPECT/MRL [7]. First, a non-contrast MRL cannot guarantee the description of the lymphatic vessels. A study of non-contrast MRL suggested that visualization of the TD was achieved in 98% of patients; however, the complete pathway was tracked in only 24% of these patients [19]. Incomplete visualization (Fig 2A) may lead to an inaccurate diagnosis; therefore, the findings of non-contrast MRL should be interpreted with caution. Second, information on dynamic imaging and the detailed anatomy of collaterals plays a pivotal role in conducting selective collateral channel embolization [11]. SPECT/MRL cannot provide this type of information. Thus, SPECT/MRL may have only a limited role in classifying the pathophysiology of lymphorrhoea. However, this fact does not undermine the importance of understanding the etiology of chylothorax because the novel classification helps to strategize lymphatic interventions [12]. Third, SPECT/MRL requires sedation several times when patients undergo CT, SPECT, or MRL, particularly in younger children. DCMRL can be performed in a single session. The examination process should be simplified as much as possible because patients with prolonged chylothorax are often clinically unstable. Considering the limitations mentioned above, SPECT/MRL does not have the potential to replace DCMRL. Nevertheless, DCMRL involves logistical and technical challenges that have hindered its use worldwide [19]. Consequently, SPECT/MRL may be an alternative to DCMRL in certain situations, especially when DCMRL is unavailable.

To our knowledge, this is the first report on the use of SPECT/MRL to diagnose a patient with chylothorax as PLPS, visualizing the TD and abnormal connections to the lung parenchyma. SPECT/MRL does not require specific skills or devices for implementation. Therefore, this modality can help elucidate the etiology of patients with lymphatic disorders when institutes cannot perform DCMRL.

In conclusion, this article highlights a case of pediatric refractory chylothorax diagnosed as PLPS based on the findings of SPECT/MRL. The anatomy of the lymphatic system and the pathophysiology of the chylothorax are essential to strategize therapeutic options. SPECT/MRL can help elucidate the etiology of chylothorax in situations where the patients are not accessible to DCMRL.

### Authors' contribution

Drs. Shima and Hara conceptualized and designed the study, drafted the initial manuscript, and reviewed and revised the manuscript; Drs. Sato and Kan were involved in the patient management, data collection, and reviewed and revised the

manuscript; Dr. Kinjo analyzed and interpreted data critically, supervised the design, and reviewed the manuscript; all authors approved the final manuscript and agreed to be accountable for all aspects of this body of work.

### Patient consent

Complete written informed consent was obtained from the patient for the publication of this study and accompanying images.

### Acknowledgement

We are deeply grateful to the members of the cardiology center, radiology, plastic surgery, and pediatric surgery for their general support and technical assistance.

### Supplementary materials

Supplementary material associated with this article can be found, in the online version, at doi:[10.1016/j.radcr.2023.01.021](https://doi.org/10.1016/j.radcr.2023.01.021).

### REFERENCES

- [1] Johnson OW, Chick JF, Chauhan NR, Fairchild AH, Fan CM, Stecker MS, et al. The thoracic duct: clinical importance, anatomic variation, imaging, and embolization. *Eur Radiol* 2016;26:2482–93. doi:[10.1007/s00330-015-4112-6](https://doi.org/10.1007/s00330-015-4112-6).
- [2] Kuo PH, Barber BJ, Kylat RI, Klewer SE, Behan S., Lau-Braunhut S, et al. Whole-body lymphangiography and SPECT/CT in children with lymphatic complications after surgery for complex congenital heart disease. *Lymphology* 2019;52:157–65.
- [3] Alejandro-Lafont E, Krompiec C, Rau WS, Krombach GA. Effectiveness of therapeutic lymphography on lymphatic leakage. *Acta Radiol* 2011;52:305–11. doi:[10.1258/ar.2010.090356](https://doi.org/10.1258/ar.2010.090356).
- [4] Rajebi MR, Chaudry G, Padua HM, Dillon B, Yilmaz S. Arnold RW, et al. Intranodal lymphangiography: feasibility and preliminary experience in children. *J Vasc Interv Radiol* 2011;22:130–5. doi:[10.1016/j.jvir.2011.05.003](https://doi.org/10.1016/j.jvir.2011.05.003).
- [5] Biko DM, DeWitt AG, Pinto EM, Morrison RE, Johnstone JA., Griffis H, et al. MRI Evaluation of lymphatic abnormalities in the neck and thorax after Fontan surgery: relationship with outcome. *Radiology* 2019;291:774–80. doi:[10.1148/radiol.2019180877](https://doi.org/10.1148/radiol.2019180877).
- [6] Dori Y, Keller MS, Fogel MA, Itkin M. MRI of lymphatic abnormalities after functional single-ventricle palliation surgery. *AJR Am J Roentgenol* 2014;203:426–31. doi:[10.2214/ajr.13.11797](https://doi.org/10.2214/ajr.13.11797).
- [7] De Angelis LC, Bellini T, Witte MH, Kylat RI, Bernas M, Boccardo F, et al. Congenital chylothorax: current evidence-based prenatal and post-natal diagnosis and management. *Lymphology* 2019;52:108–25.
- [8] Chavhan GB, Amaral JG, Temple M, Itkin M. MR lymphangiography in children: technique and potential

- applications. *Radiographics* 2017;37:1775–90. doi:10.1148/rg.2017170014.
- [9] Rocha G. Pleural effusions in the neonate. *Curr Opin Pulm Med* 2007;13:305–11. doi:10.1097/MCP.0b013e3281214459.
- [10] Biko DM, Johnstone JA, Dori Y, Victoria T, Oliver ER, Itkin M. Recognition of neonatal lymphatic flow disorder: fetal MR findings and postnatal MR lymphangiogram correlation. *Acad Radiol* 2018;25:1446–50. doi:10.1016/j.acra.2018.02.020.
- [11] Dori Y, Keller MS, Rome JJ, Gillespie MJ, Glatz AC, Dodds K, et al. Percutaneous lymphatic embolization of abnormal pulmonary lymphatic flow as treatment of plastic bronchitis in patients with congenital heart disease. *Circulation* 2016;133:1160–70. doi:10.1161/circulationaha.115.019710.
- [12] Savla JJ, Itkin M, Rossano JW, Dori Y. Post-operative chylothorax in patients with congenital heart disease. *J Am Coll Cardiol* 2017;69:2410–22. doi:10.1016/j.jacc.2017.03.021.
- [13] Ohuchi H. Where is the "optimal" Fontan hemodynamics? *Korean Circ J* 2017;47:842–57. doi:10.4070/kcj.2017.0105.
- [14] Ramirez-Suarez KI, Tierradentro-Garcia LO, Smith CL, Krishnamurthy G, Escobar FA, Otero HJ, et al. Dynamic contrast-enhanced magnetic resonance lymphangiography. *Pediatr Radiol* 2022;52:285–94. doi:10.1007/s00247-021-05051-6.
- [15] Book WM, Gerardin J, Saraf A, Marie Valente A, Rodriguez F 3rd, et al. Clinical phenotypes of Fontan failure: implications for management. *Congenit Heart Dis* 2016;11:296–308. doi:10.1111/chd.12368.
- [16] Lo Rito M, Al-Radi OO, Saedi A, Kotani Y, Ben Sivarajan V, Russell JL, et al. Chylothorax and pleural effusion in contemporary extracardiac fenestrated Fontan completion. *J Thorac Cardiovasc Surg* 2018;155:2069–77. doi:10.1016/j.jtcvs.2017.11.046.
- [17] Madru R, Kjellman P, Olsson F, Wingårdh K, Ingvar C, Ståhlberg F, et al. 99mTc-labeled superparamagnetic iron oxide nanoparticles for multimodality SPECT/MRI of sentinel lymph nodes. *J Nucl Med* 2012;53:459–63. doi:10.2967/jnumed.111.092437.
- [18] Hoogendam JP, Zweemer RP, Hobbelenk MG, van den Bosch MA, Verheijen RH, Veldhuis WB, et al. 99mTc-Nanocolloid SPECT/MRI fusion for the selective assessment of nonenlarged sentinel lymph nodes in patients with early-stage cervical cancer. *J Nucl Med* 2016;57:551–6. doi:10.2967/jnumed.115.164780.
- [19] Gooty VD, Veeram Reddy SR, Greer JS, Blair Z, Zahr RA, Arar Y, et al. Lymphatic pathway evaluation in congenital heart disease using 3D whole-heart balanced steady state free precession and T2-weighted cardiovascular magnetic resonance. *J Cardiovasc Magn Reson* 2021;23:16. doi:10.1186/s12968-021-00707-6.